Proceedings of the XVII ECSMGE-2019
Geotechnical Engineering foundation of the future
ISBN 978-9935-9436-1-3

doi: 10.32075/17ECSMGE-2019-0162

XVII European Conference
ECSMGE 2019
Reykjavík
on Soil Mechanics
and Geotechnical Engineering

Lateral stress measurement in DSS testing

Mesures de contrainte latéral en essai de cisaillement sample direct

C. Zwanenburg
Deltares – Delft University of Technology, Delft, The Netherlands

D.A. de Lange, J.A.M. Teunissen
Deltares, Delft, The Netherlands

ABSTRACT: This paper discusses the improvement of a large direct simple shear, DSS, box to measure the horizontal, out of plane, stress development during direct simple shear testing. Tests are conducted on remoulded Oostvaardersplassen-clay, OVP clay specimen with dimensions 0.26 (l) × 0.08 (h) × 0.22 (w) m. Perpendicular to the shearing direction 8 stress transducers, 4 on each sidewall are applied. Details of the set-up are described in the paper. Horizontal stress measurements are compared to finite element simulations, considering different material models. Conventional triaxial compression and triaxial extension tests have been conducted on the same material. The results of the conventional tests and the DSS tests, with horizontal stress measurement, are plotted in the deviator-plane, showing good agreement to the Matsuoka – Nakai criterion.

RÉSUMÉ: Ce papier traite de l'amélioration d'une grande boite de cisaillement simple direct pour mesurer le développement de la contrainte horizontal, hors plan, lors de l'essai du cisaillement simple direct. Les essais sont effectués sur de l'argile OVP Oostvaardersplassen remodelée avec des dimensions de 0,26 (l) × 0,08 (h) × 0,22 (w) m. Perpendiculaire au sens de cisaillement, 8 transducteurs de contrainte, 4 sur chaque paroi latérale sont appliqués. Les détails de la configuration sont décrits dans le papier. Les mesures de contraintes horizontales sont liées à des simulations d'éléments finis, en considérant différents modèles de matériaux. Des essais classiques de compression triaxiale et d'extension triaxiale ont été réalisés sur le même matériau. Les résultats des tests conventionnels et des essais de cisaillements direct, avec mesure des contraintes horizontales, sont tracés dans le plan déviatorique, ce qui montre un bon accord avec le critère de Matsuoka - Nakai.

Keywords: experimental soil mechanics; laboratory testing; direct simple shear, numerical analysis; deviator plane; soft soil behaviour

1 INTRODUCTION

Conventional laboratory testing uses axial symmetric samples, while the majority of design calculations consider plane strain conditions. It is generally acknowledged that the difference in stress conditions between axial symmetric and plane strain results in a different stress behaviour. For example Wroth (1984) suggest $\varphi'_{ps} = 9/8\ \varphi'_{txc}$, with φ'_{ps} the friction angle for plane strain conditions and φ'_{txc} the friction angle for triaxial compression strength. Despite these differences, in engineering practice the strength characteristics for general, plane strain, calculations are based on axial symmetric laboratory tests. One of the main reasons for this is the ex-

perimental difficulty encountered when conducting laboratory tests for plane strain conditions. This study explores the possibilities of improving an existing large shear box to measure horizontal stresses. Tests are conducted on remoulded Oostvaardersplassen clay, see next section and results compared to numerical simulations. Finally, the results are plotted in the deviator-plane. To support the construction of the yield contour in the failure plane, conventional triaxial undrained compression and extension tests are conducted.

2 TESTED MATERIAL

The clay was retrieved at Oostvaardersplassen, approximately 50 km north east of Utrecht, The Netherlands. The Oostvaardersplassen clay, OVP clay, is tested for natural and remoulded conditions in previous studies. Tichelaar et al. (2002) describe OVP clay as an highly active, highly organic, highly plastic clay with an organic content of 9.5% and $CaCO_3$-content of 9.2%.

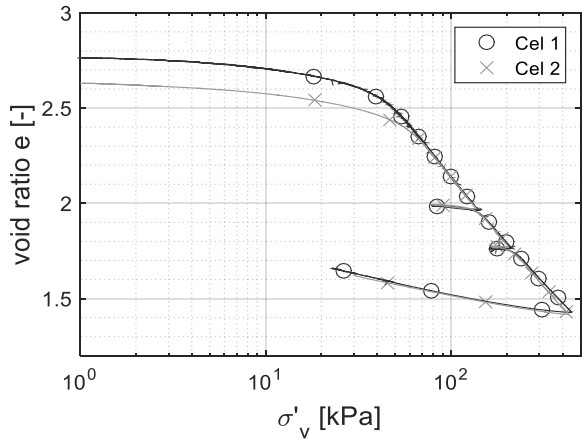

Figure 1. Constant Rate of Strain tests on remoulded OVP clay for batch 1 and 2.

This study uses remoulded specimens. The clay is mixed with water (under vacuum) to a water content, w of 181 % and consolidated for 172 days under 40 kPa. The clay is prepared in two batches, cell 1 and cell 2. Characteristics are shown by Table 1. Figure 1 shows the results of constant rate of strain, CRS test on a specimen from each of the batches. For cell 1, some problems in stress control during the consolidation period did occur, leading to a larger void ratio e_0 and a lower preconsolidation stress in cell 1, see Fig. 1.

Table 1. Characteristics of the tested specimens

Parameters	Cell 1	Cell 2
initial void ratio e_0 [-]	2.77	2.60
water content, w [%]	113.9	107.0
dry weight, γ_{dry} [kN/m^3]	6.1	6.4
saturated weight, γ_{sat} [kN/m^3]	13.1	13.3
Compression index C_c [-]	1.24	1.22

Atterberg limits were determined, using the casagrande method for measuring the liquid limit, w_l, resulting in w_l = 165.5%; plastic limit, w_p = 55.5%, and plasticity index I_p = 110 %.

3 TESTING PROGRAMME

The testing programme consisted of conventional triaxial tests, conventional and large sized direct simple shear tests, DSS and LDSS tests. The triaxial tests were used for establishing the location of the compression and extension strength in the deviator plane. The conventional sized DSS tests were used to compare results with the LDSS tests and are not further discussed in the paper.

The conventional tests have been conducted on normally and overconsolidated samples. This paper concentrates on the normally consolidated tests. Table 2 gives an overview of the triaxial tests. The samples were consolidated under K_0 stress conditions. These conditions were reached by gradually increasing the cell pressure, with 0.18 kPa/h until σ'_h = 30 kPa while controlling the vertical stress such that the radial strain remains negligible $\varepsilon_r < 0.04\%$. This resulted in σ'_v = 75 kPa and consequently K_0 = 0.4. Figure 2 shows the ratio of horizontal and vertical effective stress, σ'_h/σ'_v, during the consolidation

phase. Application of Jacky's formula results in an estimate for the friction angle, $\varphi' = 36.9°$.

OVP-clay is sensitive for creep and creep rates prior to shearing will influence the undrained shear strength gained in the shearing phase. Table 2 provides the sample properties prior to shearing.

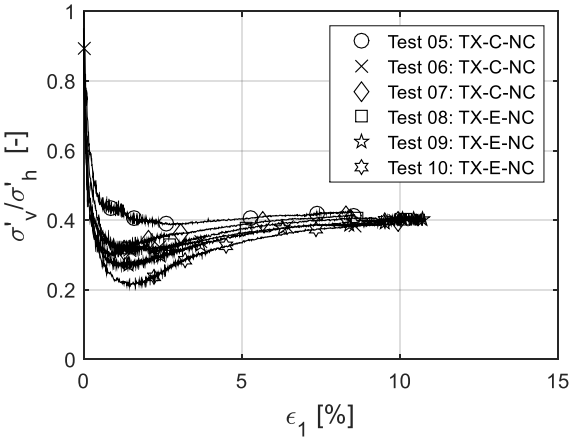

Figure 2. Development of coefficient of lateral earth pressure during the consolidation phase

Table 2. Sample conditions prior to shearing, CUC = consolidated undrained triaxial compression test, CUE = consolidated undrained triaxial extension test

No.	type	dε/dt [%/h]	*w* [%]	ρ_n [kg/m^3]
5	CUC	0.033	100.1	1410
6	CUC	0.018	98.8	1414
7	CUC	0.036	99.9	1430
8	CUE	0.028	98.9	1403
9	CUE	0.009	96.9	1419
10	CUE	0.028	95.9	1418

Figure 3 shows the resulting stress paths. CUC test number 6 differs slightly from the other 2 CUC tests, nr 5 and 7, which is explained by a minor deviation in the applied loading path resulting in a small over –consolidation, OCR = 1.04 and reduced creep rate prior to shearing, see table 2.

For test 9 a longer period between reaching the consolidation stresses and the start of the shearing phase was applied resulting in a lower creep rate compared to the fellow CUE tests, as shown by table 2. This resulted in slightly different strength behaviour.

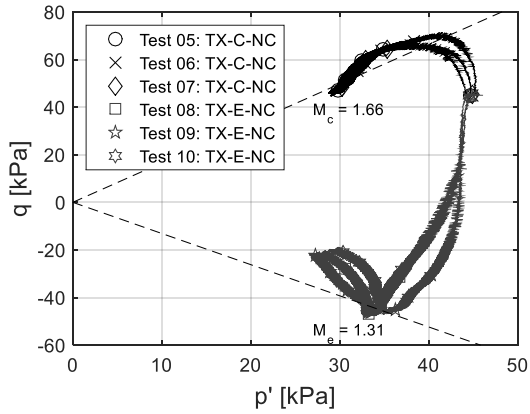

Figure 3. Effective stress paths during undrained triaxial shear

The CUC tests failed in bulging, while CUE tests failed by necking. Figure 3 shows the critical state line slope in compression, $M_c = 1.66$, resulting in $\varphi'_{cs} = 40.45°$, which is larger than obtained from the K_0-value. For the slope of the critical state line in extension, M_e is found, $M_e = 1.31$.

4 LDSS TESTS

Boxed shaped soil samples of 26 cm in length, shearing direction, 22 cm in width and 6-12 cm in height can be tested in the large direct simple shear apparatus, LDSSA. The test apparatus is described in Den Haan & Grognet (2014). Five tests on normally consolidated samples are performed: three undrained, constant volume and two drained, constant vertical stress and low shear rate. The samples are consolidated under a vertical stress $\sigma'_v = 75$ kPa. The applied shearing rate = 3%/h for the undrained tests and 0.2 %/h for the drained tests. Table 3 provides the sample properties prior to shearing. The initial sample height was 9 cm, while the height during shearing was around 8 cm. During consolidation

and shearing, the LDSSA-box is filled with water. Figures 4 and 5 show the tests results.

Table 3. Sample conditions prior to shearing,

nr	type	dε/dt [%/h]	w [%]	ρ_n [kg/m^3]
11	NCU	0.026	113.9	1384
12	NCU	0.013	113.5	1385
25	NCU	0.035	109.7	1384
23	NCD	0.037	110.2	1399
24	NCD	0.015	113.1	1391

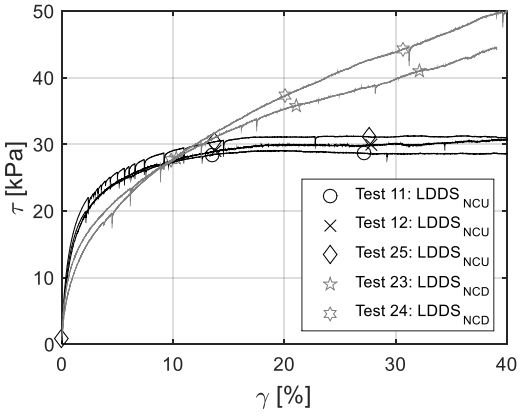

Figure 4. LDSS test results shear stress as function of shear strain

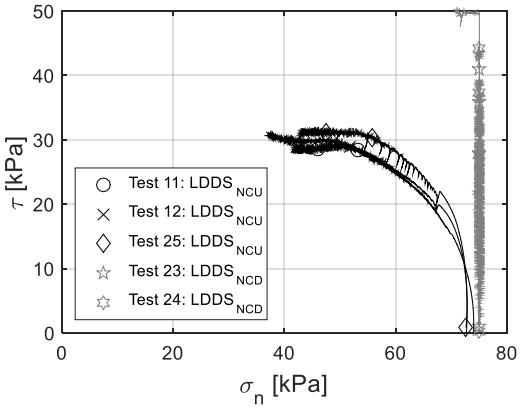

Figure 5. Shear stress as function of normal stress during shearing

5 HORIZONTAL STRESS MEASUREMENT

In order to measure horizontal stress during shearing, eight FlexiForce A201 Sensor 1lb are placed with tape at the inner side of the side walls of the LDSSA- box, see Figure 6. The diameter of the sensing area of the sensors is 9.53 mm and the sensors have a thickness of 0.21 mm. At each side wall, four sensors are placed, see Figure 6 for the locations of the sensors with respect to the sample. After placing the sensors, also a mylar sheet is placed to the walls in order to take the shear force, since the FlexiForce sensors react on both shear and normal stress. The mylar is applied to filter the shear stress. Prior to each test, the sensors are calibrated. According to the supplier, the sensors are linear within +/- 3%, the hysteresis is typically less than 4.5% and the drift is less than 5% per log of time.

Figure 7 shows the average of the horizontal stress measured by the individual sensors during the shear phase of the three tests. Especially the first sensors, sensor nr 1 and 8 tend to produce readings that differ from readings of the other sensors.

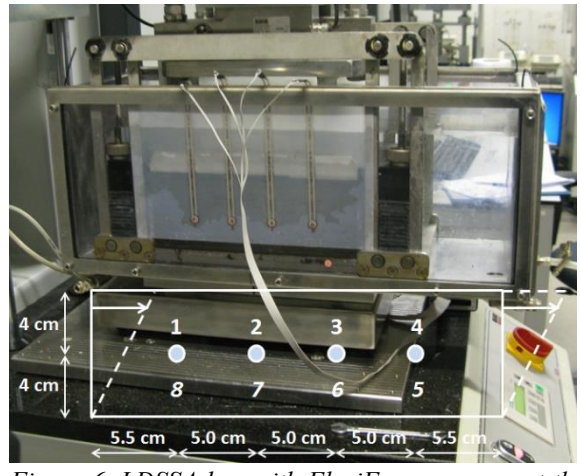

Figure 6. LDSSA-box with FlexiForce sensors at the side walls

Conventional laboratory testing yields $K_{0,nc}$ = 0.4, see Figure 2. With a vertical consolidation stress, σ'_{vc} = 75 kPa, which brings the sample in

normally consolidated conditions, the horizontal stress at the start of the shearing phase is expected to be $\sigma'_{hc} = 0.4 \times 75 = 30$ kPa. This value complies well with the initial value measured in test 12, 24 and 25. The measurements of test 11 deviate clearly from the expected value. In test 11, the first LDSS test, the sample was placed followed by installing the side walls. As a consequence the sample was slightly compressed in horizontal direction leading to horizontal stresses that clearly exceed K_0 - conditions. For the other tests, the walls were installed first and then the sample was placed. Placing the sample was facilitated by trimming the sample slightly smaller than the shear box. During the consolidation phase the specimen settles against the sidewalls reaching K_0 stress conditions.

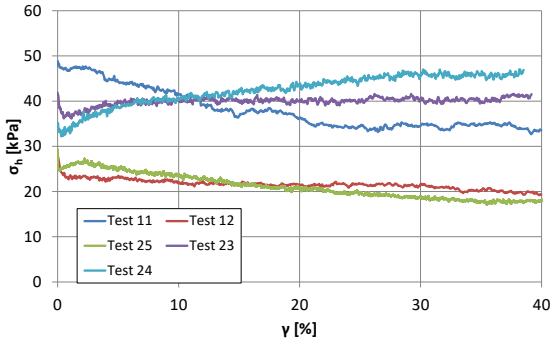

Figure 7. Measured horizontal stress during shear phase

During shearing, the horizontal stress in the undrained tests 12 and 25 shows an initial rapid drop followed by a nearly constant development or a small decline afterwards. Figure 5 shows that for the undrained tests the vertical effective stress the vertical effective stress reduces to approximately $\sigma'_v = 40$ kPa. Consequently the ratio σ'_h / σ'_v increases from initially 0.4 to finally 0.5.

For the drained tests, the ratio σ'_h / σ'_v reaches 0.5 to 0.6 at the end of the test.

6 NUMERICAL SIMULATIONS

To increase the understanding of the LDSS test results including the horizontal stress development a series of numerical simulations were conducted, using the Soil Test module, PLAXIS, version 2017 (PLAXIS 2016). Simulations were made using the soft soil, SS model, soft soil creep, SSC model and the Creep SCLAY1 model. The SS and the SSC model are standard available in the computer programme (PLAXIS, 2016). The Creep SCLAY1 model is applied as a user-defined model. It is beyond the context of this paper to fully describe this model. Details of the model can be found in a.o. Wheeler et al, (2003), Grimstad et al (2010), Sivasithamparam (2012) and (2015). For this paper the Creep SCLAY1 implementation provided by Deltares[1], has been used.

All three models are Cam Clay-type models with an increase in complexity, with SSC model allowing for creep and Creep-SCLAY1 model allowing for plastic anisotropy and creep. The applied parameters are described in Zwanenburg et al. (2018). The stiffness parameters are derived from simulating the CRS tests shown in Figure 1. The strength parameters are obtained from triaxial compression test results, Figure 3.

Figure 8 shows a typical stress development found in a SSC simulation of undrained DSS test. During shear, the vertical stress decreases while the horizontal stress in shearing direction increases untill both are equal. The horizontal stress perpendicular to shearing shows a minor decline. For drained shearing the vertical stress remains constant, while horizontal stress increases but will not reach the level of vertical stress before the maximum shear strain of 40% is reached.

Figure 9 shows the comparison of the measured shear stress, τ and shear strain γ to numerical simulations. The Soft Soil Creep model shows some softening after reaching a peak val-

[1] free downloadable through: https://www.deltares.nl/en/deltares-creep-sclay1/.

ue. This numerical behaviour is explained by creep that results in the numerical simulations in relaxation.

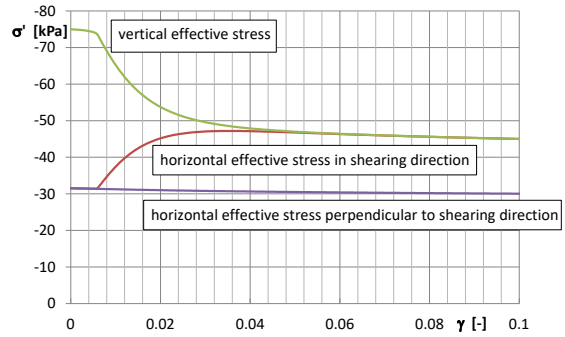

Figure 8, Soft Soil Creep simulation of the stresses during undrained simple shear

In general, the numerical simulations seem to react too stiff, with the maximum shear strength reached at $\gamma = 0.02$, while the measurements reach a maximum shear strength at $\gamma = 0.2$. The Creep SCLAY1 model is able to predict the stress strain behaviour in Figure 9.

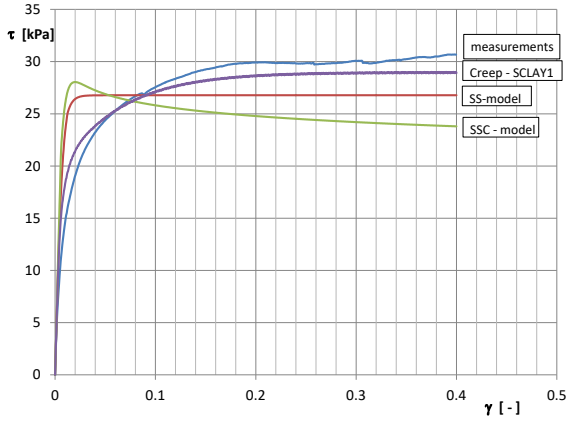

Figure 9, Simulation of test 12, undrained test, with different material models, shear stress versus shear strain

Figures 10 and 11 compare the measured horizontal stress development to the simulation results. As to be expected the initial value of the horizontal stress start at K_0 conditions. For the constant volume test, test 12, the horizontal stress measurement shows an initial drop followed by approximately constant development. It is remarkable that the soft soil model predicts equivalent behaviour, while the SSC model predicts a gradual decline, without an initial drop. The Creep SCLAY1 model predicts the initial drop in horizontal effective stress, however this drop is followed by a gradual increase which is not found in the measurements.

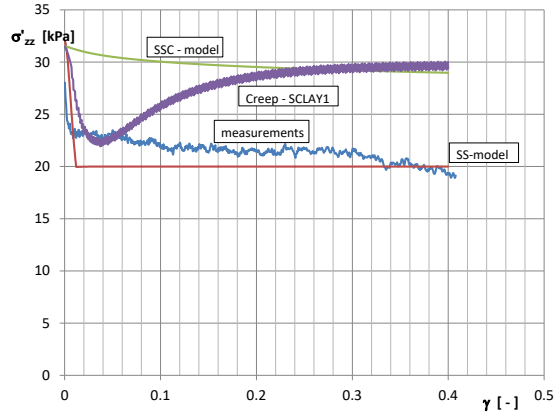

Figure 10, Simulation of horizontal stress, perpendicular to shearing for undrained Test 12

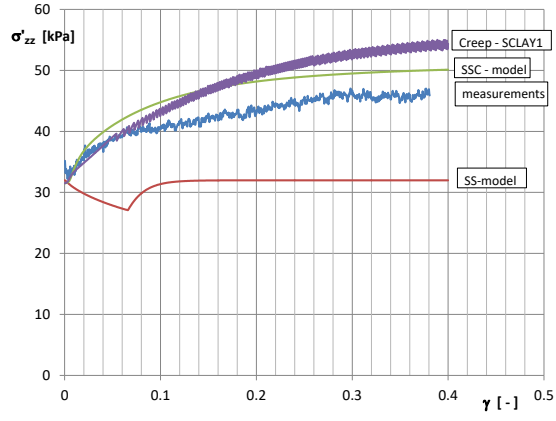

Figure 11, Simulation of horizontal stress, perpendicular to shearing for drained Test 24

For drained test 24, Figure 11, a gradual increase in horizontal effective stress is found in both measurements as in the SSC and Creep SCLAY1 simulations. The SS simulation shows

a constant effective horizontal stress at about K_0 conditions.

7 DEVIATOR PLANE

In order to plot the data in the deviator plane the following assumptions are required:

- The measured, horizontal stress equals the intermediate principal stress, σ'_2
- At critical state the combination of τ and σ'_v corresponds to the top of the Mohr Circle, implying vertical effective stress being equal to the horizontal effective stress in shearing direction, as found in Figure 8.
- For undrained testing these stress conditions are reached rapidly, while for the drained tests it is questionable if these conditions are reached before terminating the tests.
- Critical state stress conditions are reached at the end of the test.

Using the assumptions given above, the principal stresses at critical state follow from:

$$\sigma'_1 = \frac{\sigma'_{xx}+\sigma'_{yy}}{2} + \sqrt{\left(\frac{\sigma'_{xx}-\sigma'_{yy}}{2}\right)^2 + \tau_{xy}^2}$$

$$\sigma'_2 = \sigma'_{zz}$$

$$\sigma'_3 = \frac{\sigma'_{xx}+\sigma'_{yy}}{2} - \sqrt{\left(\frac{\sigma'_{xx}-\sigma'_{yy}}{2}\right)^2 + \tau_{xy}^2}$$

In which σ'_{xx} represents the horizontal stress in shear direction, σ'_{yy} the vertical effective stress, σ'_{zz} the effective out of plane horizontal stress and $\sigma'_{1,2,3}$ the principal effective stresses Table 4 summarizes the critical state conditions observed in the 5 LDSS tests. The relative magnitude of the intermediate stress is given by the ratio $b = (\sigma_2 - \sigma_3)/(\sigma_1 - \sigma_3)$.

Table 4, Stress conditions at critical state, [1] = undrained test, [2] = drained test. b = parameter for intermediate stress.

nr	σ'_v [kPa]	τ_{xy} [kPa[	σ'_{zz} [kPa]	b [-]
11[1]	41.76	28.61	33.54	0.36
12[1]	37.18	30.67	26.27	0.32
25[1]	42.87	30.96	17.94	0.10
23[2]	75.00	44.50	41.55	0.12
24[2]	75.00	49.67	43.03	0.18

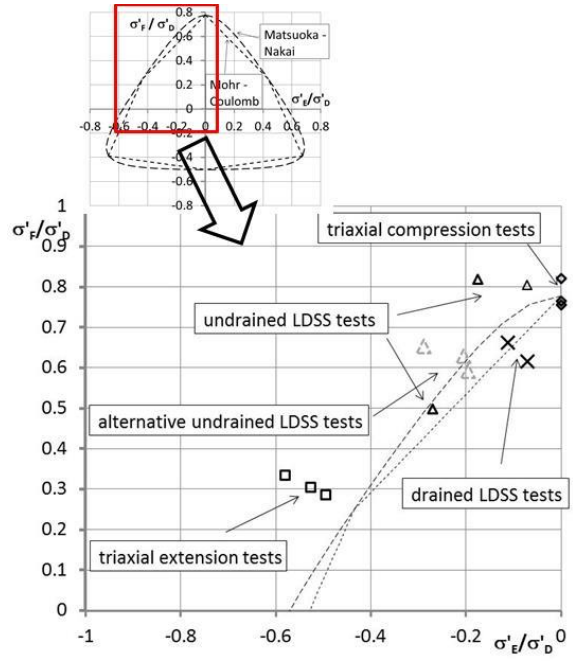

Figure 12 Results plotted in deviator-plane

Figure 12 compares the test data to the Mohr Coulomb and Matsuoka – Nakai criteria, for φ'_c = 40.3°, which corresponds to M_c = 1.66 found by Figure 3. To plot the 3D contour the procedure given by Davis & Selvadurai (2002) is followed, in which $\sigma'_D = (\sigma'_1 + \sigma'_2 + \sigma'_3)/\sqrt{3}$, $\sigma'_E = (-\sigma'_2 + \sigma'_3)/\sqrt{2}$, $\sigma'_F = (2\sigma'_1 - \sigma'_2 - \sigma'_3)/\sqrt{6}$.

The results for the triaxial extension tests lay outside both criteria. This might be explained by the failure conditions for the extension tests, which failed by necking, making a proper estimate of the stress conditions at critical state complex. The test results, especially for the un-

drained tests lay relatively high, close to the triaxial compression results. The drained tests result in slightly lower strengths which might result from the low shear strain rate applied in the drained tests. Discussion was raised on the initial drop in measured horizontal stress. Some numerical simulations suggest that for undrained shearing the out of plane stress remains equal to its initial, $K_{0,}$ value. These stress conditions are depicted by the dotted triangles in Figure 12.

8 CONCLUSIONS

A large direct simple shear box is extended by pressure transducers to measure the horizontal stress perpendicular to the shearing direction. Tests for drained and undrained shearing conditions have been conducted.

As is to be expected the initial horizontal stress complies with the K_0 value observed in the conventional laboratory testing. Upon shearing, the undrained tests show an intial rapid drop after which the horizontal stress remains constant or slightly declines. For drained tests, the horizontal stress monotonically increases during shearing.

The different material models shows differences in predicted horizontal stress. The soft soil creep model and Creep SCLAY1 model seem to correctly predict the trend in horizontal stress development for the drained tests. However, these models seem to overestimate the horizontal stress development for undrained test. In contrast the soft soil model predicts a correct trend in horizontal stress development for the undrained tests and underestimates the horizontal stress development during drained shearing.

For a full independent estimation of the three dimensional stress conditions during shear, information on the horizontal stress development in shearing direction is required as well. Hopefully, in future research further improvements of the device, to measure the horizontal stress in shearing direction, will be made.

9 ACKNOWLEDGEMENTS

The authors would like to acknowledge Rijkswaterstaat and waterschap Rivierenland for supporting this research through the POVM research programme.

10 REFERENCES

Davis, R.O., Selvadurai, A. P. S. (2002). Plasticity and Geomechanics. Cambrigde University Press.

Den Haan E.J., Grognet M. (2014) A large direct simple shear device for the testing of peat at low stresses *Géotechnique Letters* **4** no 4 p. 283 - 288

Grimstad G., Degago S., Nordal S., Karstunen M. (2010) Modelling creep and rate effects in structured anisotropic soft clays *Acta Geotechnica,* vol. 5, pp. 69-81

PLAXIS (2016) Manual

Sivasithamparam N., (2012) Modelling Creep Behaviour of Soft Soils, *report PLAXIS b.v. & University of Strathclyde*

Sivasithamparam N., Karstunen M., Brinkgreve R., Bonnier P. (2013) Comparison of two anisotropic creep models at element level. in: *International Conference on Installation Effects in Geotechnical Engineering*, Rotterdam

Wroth C.P. (1984) The interpretation of in situ soil tests *Géotechnique* **34** no 4 p 449-489

Wheeler S.J., Näätänen A., Karstunen M., Lojander M. (2003) An anisotropic elastoplastic model for soft clays *Can. Geotech. J.,* vol. 40, p. 403, 2003

Zwanenburg C., De Lange D.A., Konstandinou M. (2018) POVM Validatie uitgangspunten en lange termijnontwikkeling, *POVM project report* 11200999-004 (in Dutch)